Cancer Letters 533 (2022) 215607

Contents lists available at ScienceDirect

Cancer Letters

journal homepage: www.elsevier.com/locate/canlet

Original Articles

TRF2 cooperates with CTCF for controlling the oncomiR-193b-3p in colorectal cancer

Roberto Dinami [a], Eleonora Petti [a], Manuela Porru [a], Angela Rizzo [a], Federica Ganci [a], Andrea Sacconi [a], Paola Ostano [b], Giovanna Chiorino [b], Livio Trusolino [c,d], Giovanni Blandino [a], Gennaro Ciliberto [e], Pasquale Zizza [a,**,1], Annamaria Biroccio [a,*,1]

[a] Oncogenomic and Epigenetic Unit, IRCCS – Regina Elena National Cancer Institute, via Elio Chianesi 53, Rome, 00144, Italy
[b] Cancer Genomics Lab, Fondazione Edo ed Elvo Tempia, via Malta 3, Biella, 13900, Italy
[c] Department of Oncology, University of Torino, Strada Provinciale 142, Candiolo, TO, 10060, Italy
[d] Laboratory of Translational Cancer Medicine, Candiolo Cancer Institute, FPO – IRCCS, Strada Provinciale 142, Candiolo, TO, 10060, Italy
[e] Scientific Direction, IRCCS - Regina Elena National Cancer Institute, via Elio Chianesi 53, Rome, 00144, Italy

ARTICLE INFO

Keywords:
TRF2
miR-193b-3p
Colorectal cancer
CTCF
Prognostic markers

ABSTRACT

The Telomeric Repeat binding Factor 2 (TRF2), a key protein involved in telomere integrity, is over-expressed in several human cancers and promotes tumor formation and progression. Recently, TRF2 has been also found outside telomeres where it can affect gene expression. Here we provide evidence that TRF2 is able to modulate the expression of microRNAs (miRNAs), small non-coding RNAs altered in human tumors. Among the miRNAs regulated by TRF2, we focused on miR-193b-3p, an oncomiRNA that positively correlates with TRF2 expression in human colorectal cancer patients from The Cancer Genome Atlas dataset. At the mechanistic level, the control of miR-193b-3p expression requires the cooperative activity between TRF2 and the chromatin organization factor CTCF. We found that CTCF physically interacts with TRF2, thus driving the proper positioning of TRF2 on a binding site located upstream the miR-193b-3p host-gene. The binding of TRF2 on the identified region is necessary for promoting the expression of miR-193b3p which, in turn, inhibits the translation of the onco-suppressive methyltransferase SUV39H1 and promotes tumor cell proliferation. The translational relevance of the oncogenic properties of miR-193b-3p was confirmed in patients, in whom the association between TRF2 and miR-193b-3p has a prognostic value.

1. Introduction

The Telomere Repeat-Binding Factor 2 (TRF2), one of the six proteins constituting the shelterin complex, takes part in the maintenance of telomere integrity and genome stability [1]. In particular, TRF2, through its binding to double-stranded telomere repeats (TTAGGG), provides a protective capping function that, suppressing DNA damage response (DDR) and non-homologous end joining (NHEJ), avoids the erroneous recognition of the terminal portions of chromosomes as sites of DNA damage [2]. In addition, TRF2 has been found to function as a topological stress sensor that counteracts telomere fragility due to the stall of the replicative fork proper of highly heterochromatic DNA regions [3].

The idea of an exclusively telomeric role of TRF2 was unhinged almost ten years ago by a pioneering study, first demonstrating the existence of extratelomeric binding-sites of TRF2: pericentromeric satellite III (sat III) sequences and interstitial telomeric sequences (ITSs), telomere-like TTAGGG sequences diffused alongside the entire genome

Abbreviations: TRF2, Telomere Repeat-Binding Factor 2; DDR, DNA damage response; ITSs, Interstitial Telomeric Sequences; miRNAs, microRNAs; CRC, Colorectal cancer; ChIP, Chromatin Immunoprecipitation; IP, Immunoprecipitation; PCR, Polymerase chain reaction; TCGA, The Cancer Genome Atlas; DFS, Disease-free survival; OS, Overall Survival; Taq-Man qPCR, Taq-Man polymerase chain reaction; SUV39H1, Histone-lysine N-methyltransferase SUV39H1; H3K9-3me, Histone H3-K9 methyltransferase 3; MDSC, Myeloid-derived suppressorcells; NK, Natural Killer; VEGF-A, Vascular endothelial growth factor A.

* Corresponding author.
** Corresponding author.
E-mail addresses: pasquale.zizza@ifo.it (P. Zizza), annamaria.biroccio@ifo.it (A. Biroccio).
[1] These authors contributed equally to this work.

https://doi.org/10.1016/j.canlet.2022.215607
Received 9 November 2021; Received in revised form 11 February 2022; Accepted 24 February 2022
Available online 28 February 2022

[4]. The discovery of these novel binding sites marked a turning point in the biology of TRF2. Indeed, through the binding to Sat III regions, TRF2 facilitates replicative fork progression also through pericentromeres, so assuming a more general role in ensuring genome-wide heterochromatic stability [5]. Moreover, studies concerning the distribution of ITSs within the genome demonstrated that these sequences are particularly abundant in the proximity of gene regulatory elements, such as promoters and/or enhancers, and that TRF2, by binding these regions, controls the expression of a number of target genes [6–12].

Interestingly, TRF2 has been found overexpressed in several human malignancies and in the vasculature of many cancer types [13–15]. TRF2 contributes to carcinogenesis in mice and is regulated by the Wnt/β-catenin pathway [16,17]. Moreover, consistently with its oncogenic role in human cancers, an increased dosage of TRF2 in a variety of tumor cells enhances their tumorigenicity, whereas TRF2 depletion reduces tumor growth [7,18–20]. Studies recently published by our and other laboratories have demonstrated that a large part of the tumor-related properties of TRF2 are essentially attributable to its capability to affect the expression of genes (*e.g.* HS3ST4, GPC6, VCAN, SULF2), mainly involved in the reorganization of cell glycocalyx [7,10,12]. Indeed, by promoting tumor immune escape and angiogenesis, TRF2-regulated genes have been demonstrated to deeply impact on the processes of tumor formation, growth and dissemination [7,10,12].

Despite the progresses done in the last few years, currently available data are still insufficient to explain at all the plethora of functions involving TRF2, indicating that our knowledge – especially that concerning the mechanisms through which TRF2 exerts its oncogenic role – is still limited and needs additional investigations.

In the last few years a growing body of literature highlighted the relevance of microRNAs (miRNAs), a class of endogenous non-coding RNAs, in physiological and pathological processes, included cancer biology [21]. Indeed, playing a pivotal role as post-transcriptional regulators of gene expression, miRNAs can act, depending on their target genes, as both tumor promoters and tumor suppressors [22,23]. Moreover, due to their key role in tumorigenesis, miRNAs have been investigated as prognostic and diagnostic biomarkers and as useful targets for therapeutic intervention [24,25].

Compelling evidence has demonstrated that miRNA expression is dysregulated in human cancer through various mechanisms, which include, among others, abnormal miRNA transcription, epigenetic changes and defects in the miRNA biogenesis machinery [26,27]. Here, we explored the possibility that TRF2 affects – similar to that already observed for protein-coding genes – also the expression of cancer-related miRNAs.

Notably, our results demonstrated that TRF2 is able to regulate the expression of a number of miRNAs, including the miR-193b-3p, a small non-coding RNA that exerts a significative oncogenic activity in colorectal cancer (CRC) by targeting the histone-lysine *N*-methyltransferase SUV39H1. Moreover, here we elucidated the mechanism through which TRF2 exerts its activity as a transcriptional regulator of miRNA expression. We showed that the control of miR-193b-3p expression is mediated by the coordinated activity of TRF2 with CTCF, a chromatin organization factor that modulates gene expression. In particular, our data demonstrated that CTCF, driving the positioning of TRF2 on the DNA, creates the proper conditions for promoting the transcriptional control of miR-193b-3p by TRF2. These data first obtained *in vitro*, also using advanced cellular models, were finally confirmed in CRC patients in whom the association between TRF2 and miR-193b-3p assumes a marked prognostic relevance.

2. Materials and methods

2.1. Biological resources

Colon cancer cell line HCT116 were purchased from ATCC. Dicer-deficient HCT116 cells ($Dicer^{Ex5/Ex5}$) were generously provided by professor Vogelstein B. (Johns Hopkins University, Baltimore, MD, USA). Human embryonic kidney cells (HEK293T) were provided by professor Gilson E. (IRCAN, Nice, France). All these cell lines were grown in high glucose Dulbecco modified eagle medium (DMEM; Invitrogen, Carlsbad, CA, USA) supplemented with L-glutamine, Penicillin/streptomycin and 10% foetal bovine serum (FBS, Hyclone). Colorectal cancer cells (HT29, SW480, SW620, HCT15 and LIM2527) were kindly provided by professor Milella M. (University of Verona, Verona, Italy) and were grown in Roswell Park Memorial Institute (RPMI) 1640 medium (Gibco) supplemented with L-glutamine, Penicillin/streptomycin and 10% foetal bovine serum (FBS, Hyclone). The CRC organoids were grown in Dulbecco's Modified Eagle's Medium/Nutrient mixture F-12 Ham (D6421, Sigma-Aldrich) supplemented with: B-27 (17504–044, GIBCO), N2-supplements (17502–048, GIBCO), *N*-acethylcysteine (A9165, Sigma-Aldrich), EGF 20 ng/ml (E9644, Sigma-Aldrich), L-glutamine, Penicillin/streptomycin and 10% foetal bovine serum (FBS, Hyclone) as previously reported [28]. Organoids cultures were maintained and passaged every 2 weeks.

2.2. Transfection and infection of cell lines

Cells were transiently transfected with the indicated mimic-miRNA (Ambion; ThermoFisher Scientific) or with the siRNA (GE Healthcare Dharmacon, Inc., Lafayette, CO, USA) by using the Interferin reagent (Polyplus, New York, NY, USA), according to the manufacturer's instructions. SUV39H1 and TRF2 over-expressing HCT116 cells were obtained by transient transfection of human HCT116 by using the JetPEI reagent (Polyplus) according to the manufacturer's instructions. All the analyses were performed 72h after cell transfection.

Stable TRF2 over-expressing HCT116 and HT29 cells and their control (pBabe-Empty) were infected with retroviral particles produced into Phoenix-AMPHO cells transfected with retroviral vectors (pBabe-puro-Empty and pBabe-puro-mycTRF2) [29]; using the JetPEI reagent (Polyplus, New York, NY, USA), according to the manufacturer's instructions.

To establish stable suppression of TRF2 gene, HCT116 and SW620 were infected with lentiviral particles produced into HEK293T cells, transfected with the packaging pCMVR8.74 and the envelope pMD2.G vectors in combination with the vectors encoding either for a scramble short hairpin sequence (shSCR; N2040 targeting E.coli DNA polymerase) or for one of the two short hairpin sequences directed against TRF2 (shTRF2_N1; N2573 TRCN0000004813 or shTRF2_N2; N2571 TRCN0000004811, which were a gift from Prof Shoeftner S. (University of Trieste, Trieste, Italy). After infection, cells underwent to antibiotic selection by incubation with puromycin. Puromycin was used at a final concentration of 0.3 μg/ml for HT29 and 1 μg/ml for HCT116 and SW620. All the analyses were performed starting from 7 days after antibiotic selection. Early passages of stably infected cells were used for all experiments.

2.3. TaqMan and Sybr green qPCR

To evaluate miRNA and gene expression by Taq-Man qPCR and Real-Time qPCR, total RNA was isolated from cell pellets by using TRIzol reagent (Ambion by ThermoFisher Scientific). For pri-miRNA, cells were lysed by using Cell Nuclear Extraction kit (Applied Biosystems by ThermoFisher Scientific), and nuclear RNAs were extracted by using TRIzol reagent. Quality (A260nm/A280nm absorbance ratio) and quantity (ng/μl) of extracted RNA was assessed by Nanodrop (Nanodrop 1000, ThermoFisher Scientific).

Specific miRNA reverse transcription (RT) was obtained using the Reverse Transcription Kit with the specific RT probe (Applied Biosystems by ThermoFisher Scientific).

For each sample 1.5 μl of specific RT was mixed with 0.75 μl of specific probe (Applied Biosystems by ThermoFisher Scientific), 7.5 μl of 2x-TaqMan fast universal PCR master mix (Applied Biosystems by

ThermoFisher Scientific) and 5.25 μl of water. Thermal parameters used: one cycle of 95 °C for 10 min then 40 cycles of 95 °C for 3 s and 60 °C for 30 s.

Reverse transcription of total RNA was performed using the QuantiTect Reverse Transcription Kit (Qiagen) according to the manufacturer's instructions. For each sample 5 μl of the 1:10 diluted cDNA was mixed with 0.5 μl of each primer (10 μM), 10 μl of the power syber green master mix (Applied Biosystems by ThermoFisher Scientific) and water at final volume of 20 μl. Standard qPCR thermal parameters were used: one cycle of 95 °C for 10 min then 40 cycles of 95 °C for 15 s and 60 °C for 1 min followed by dissociation curve (95 °C for 15 s, 60 °C for 1 min, 95 °C for 15 s). Both qPCRs were performed using QuantStudio 6-Flex (ThermoFisher Scientific) or 7900HT Fast Real-Time PCR System (Applied Biosystems).

The primers used for gene analysis were synthesized by Integrated DNA Technologies (BVBA Leuven, Belgium) or Metabion international AG. For each primers' pair, forward and reverse sequences are specified in the Supplementary Table 1. All experiments were run in triplicate and the gene expression levels were calculated using the 2^(-ΔΔCt) method. The gene expression was normalized to β-actin, 18S for pri-miR-193b levels or RNU44 for miR-193b expression.

2.4. Western blotting

Western blot analysis was performed as previously reported [30]. Expression levels of TRF2 and SUV39H1 were evaluated by using the mouse anti-TRF2 (4A794; Millipore) and the mouse anti-SUV39H1 (C-10; Santa Cruz Biotechnology Inc., CA, USA). The RISC complex was evaluated by using the following antibodies: rabbit anti-Dicer (30226; Santa Cruz Biotechnology Inc.); rabbit Drosha (3364; Cell Signaling, Beverly, MA, USA); mouse Ago2 (2897; Cell Signaling). Samples were normalized by using mouse β-actin (Sigma) and mouse HSP72/73 (Calbiochem, EMD Bioscience, La Jolla, CA, USA) antibodies.

2.5. Chromatin immunoprecipitation (ChIP) assay

ChIP assay was performed as reported in Ref. [12]. Briefly, for each condition 7×10^5 HCT116 cells were plated and, after 72h, fixed with 1% of formaldehyde. Nuclei were lysed with SDS lysis buffer using a Dounce homogenizer with B pestle (tight) 5 times. Next, the lysates were sonicated 3 times for 5 min setting high level by using the biorupter standard (Diagenode Inc., NXT-Dx Belgium). The average length of sonicated chromatin was around 300–400 bp. For each immunoprecipitation condition 100 μg of chromatin and 5 μg of the indicated antibodies were used. The antibodies used for the immunoprecipitation are: rabbit TRF2 (NB110-57130, Novus), rabbit CTCF (C15410210-50, Diagenode), IgG Rabbit (Bethyl).

The primers are reported in the Supplementary Table 1. All the qPCRs were performed using Power SYBR Green Master Mix (Applied Biosystems by ThermoFisher Scientific) in the QuantStudio 6-Flex (ThermoFisher Scientific) or in the 7900HT Fast Real-Time PCR System (Applied Biosystems). ChIP analysis was performed using the percent Input method.

2.6. Immunoprecipitation (IP) and pull-down assay

HCT116 cells were lysed by using a sequential lysis buffer A (10 mM Hepes pH 7.9, 10 mM KCl, 0.1 mM EDTA, 0.1 mM EGTA, 0.6% NP-40, 1 mM DTT and 1 mM PMSF) and buffer C (20 mM Hepes pH 7.9, 400 mM NaCl, 0.1 mM EDTA, 0.1 mM EGTA, 1 mM DTT and 1 mM PMSF), which resulted in cytosolic and nuclear fraction isolation respectively. Protein concentration was determined and 500 μg of nuclear fraction were used for each IP.

For IP, magnetic beads A and G (Dynabeads, ThermoFisher Scientific) were washed with PBS with 0.02% Tween 20 (Wash Buffer) and bound to 4 μg of mouse anti-TRF2 (4A794; Millipore) or rabbit CTCF (Diagenode) antibodies and mouse IgG or rabbit as negative control (15 min of incubation at RT). Next, antibodies bound to the magnetic beads were washed and incubated with nuclear extracts for 45 min at RT. Immunoprecipitates were washed, eluted from the magnetic beads with 4× Laemmli Sample Buffer, and boiled at 95 °C for 5 min before SDS page.

For the pull-down assay, 400 μg of nuclear extracts were incubated 16h at 4 °C with 30 μl of recombinant protein-conjugated resin in a buffer containing 50 mM Tris–HCl pH 7.5, 150 mM NaCl, 5 mM EDTA, 0.1% NP-40, 1 mM DTT and 1 mM PMSF. After five washes with a buffer containing 50 mM Tris-HCl pH8, 200 mM NaCl, 0.25% NP-40 and 0.5 mM PMSF, beads were resuspended in 20 μl of reducing protein loading buffer and incubated at 95 °C for 5 min. Supernatant was run on a denaturating SDS page. Signal of CTCF was revealed by Western blot analysis by using the antibody against CTCF (C15410210-50, Diagenode).

2.7. Cell proliferation

HCT116 (10×10^3 cells/well in 24 well plates) 72h post-transfection with the indicated mimic-miRNAs, alone and in combination with SUV39H1 or its relative empty vector, were seeded.

The confluence of the cells was monitored using the IncuCyte S3 (Sartorius) every 24h for a total of four days. The phase-contrast images were acquired using a 10× objective and 9 photos for each well were snap to the indicated time. The analysis was performed with the specific software IncuCyte Live-Cell analysis system (Sartorius).

2.8. Time-lapse microscopy

CRC organoids were resuspended in cultrex reduced growth factor BME type 2 and drops of 100 μl were plated into chamber slides (15 μ-Slide 4 well glass bottom, Ibidi). Then, organoids were transfected with 50 nM of the indicated mimic-miRNAs (following the protocol already reported for 2D cell lines). The day after, 4-well slides were loaded into a specific chamber (5% CO_2 and 37 °C) and phase-contrast images were acquired at time 0 and after 96h using the microscope Leica DMi8 (20× objective). The software used to set the parameters was LasX (Leica).

2.9. Cloning 3′UTR-SUV39H1 into dual luciferase vector

The region containing the two putative binding sites of miR-193b-3p into the 3′UTR of SUV39H1 was first amplified from genomic DNA using PCR Kapa HiFi HotStart 2x (KapaBiosystems) with the primers reported in Supplementary Table 1. The thermocycler was set with the following stages:

1. 95 °C 3min,
2. 98 °C 20 s, 61 °C 15 s and 72 °C 1.20 s for 3 cycles.
3. 98 °C 20 s, 70 °C 15 s and 72 °C 1.20 s for 25 cycles.
4. 72 °C 2 min

The PCR was analysed by agarose gel, the band was cut and purified using the gel extraction kit (Qiagen). Next, the PCR fragments and the PsiChek2 vector (Promega) were digest at 37 °C for 1h using *Not*I and *Xho*I enzymes (NEB). Finally, the 3′UTR of SUV39H1 was cloned into PsiChek2 vector using the T4 ligase reaction (NEB) at 16 °C for 16h.

2.10. Luciferase assay

HeLa cells were seeded (3×10^3 cells/well) in 96 well plates, next day cells were transient transfected with the indicated mimic-miRNAs (10 nM). After 24h, HeLa cells were transfected with the dual luciferase PsiChek2 (Promega) vector in which was cloned the 3′UTR of SUV39H1 wt (downstream the Renilla gene) or the 3′UTR of SUV39H1 deleted (del) for the putative binding sites of miR-193b-3p. Three days

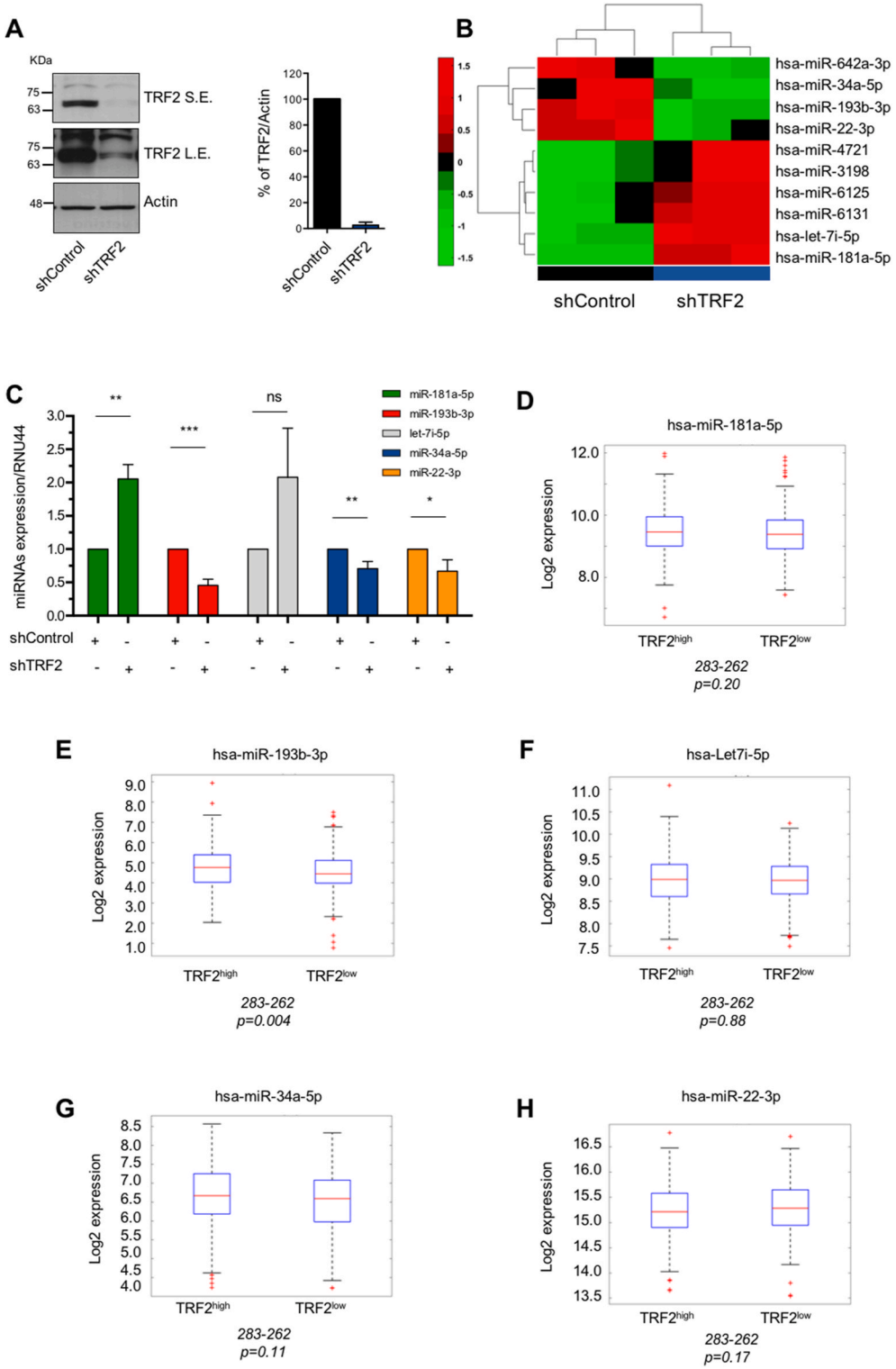

Fig. 1. TRF2 regulates miRNAs expression in colon cancer. (A) Western blot analysis of TRF2 levels in HCT116 cells stably silenced for TRF2 or its control counterpart (shControl). Left panel: representative images showing the expression levels of TRF2 (S.E. short exposure; L.E. long exposure). Actin levels were evaluated as loading control. Right panel: quantification of TRF2 expression normalized to Actin levels. Histograms show the mean (±SD) of at least three independent experiments. (B) microRNA expression profiling analysis was performed in TRF2-compromised (shTRF2) HCT116 cells derived from (A). Unsupervised hierarchical clustering was used for the analysis. miRNAs significantly regulated by TRF2 are shown. (C) Selected miRNAs identified in (B) were validated by TaqMan qPCR in HCT116 cells silenced for TRF2 (shTRF2) in comparison with their control counterpart (shControl). RNU44 was used as normalization control of miRNAs expression. The histogram shows the mean (±SD) of three independent experiments performed in triplicate. The p-values (*P < 0.1, **P < 0.01, ***P < 0.001; Student's t-test) are shown (D–H) A cohort of 621 CRC patients from the TCGA dataset were used to analysed the clinical relevance of miRNAs validated in (C). CRC patients were stratified on the basis of TRF2 levels (high or low) and miRNA expression was evaluated. The high or low TRF2 subgroups were defined considering positive and negative z-scores of TRF2 expression, respectively. On each box, the central mark is the median, the edges of the box are the 25th and 75th percentiles and the outliers are plotted individually. Statistical significance between distributions of miRNAs in high and low TERF2 patients was assessed by two-sided Wilcoxon rank sum test. P-values are reported in the figure.

after the mimic-miRNAs transfection, the cells were assay by using the Dual-Glo® Luciferase reagents (Promega) and the plates were read by luminometer. The values were normalized using the PsiChek2-Empty or the 3′UTR-SUV39H1 del vectors in combination with the mimic-miR-Control.

2.11. Microarray data analysis

The signals of 2006 human miRNAs from Agilent array platform for TRF2-silenced HCT116 cells and their controls were verified for quality control and extracted by Agilent Feature Extraction 10.7.3.1 software. The arrays were quantile normalized.

All values lower than 1 were considered below detection (threshold set to 1) and data were log2-trasformed. miRNAs not expressed were excluded. After normalization and filtering 162 expressed miRNAs were considered for further analyses.

Differential expression between subgroups of samples was assessed by a Student's t-test and a permutation test. miRNAs significantly

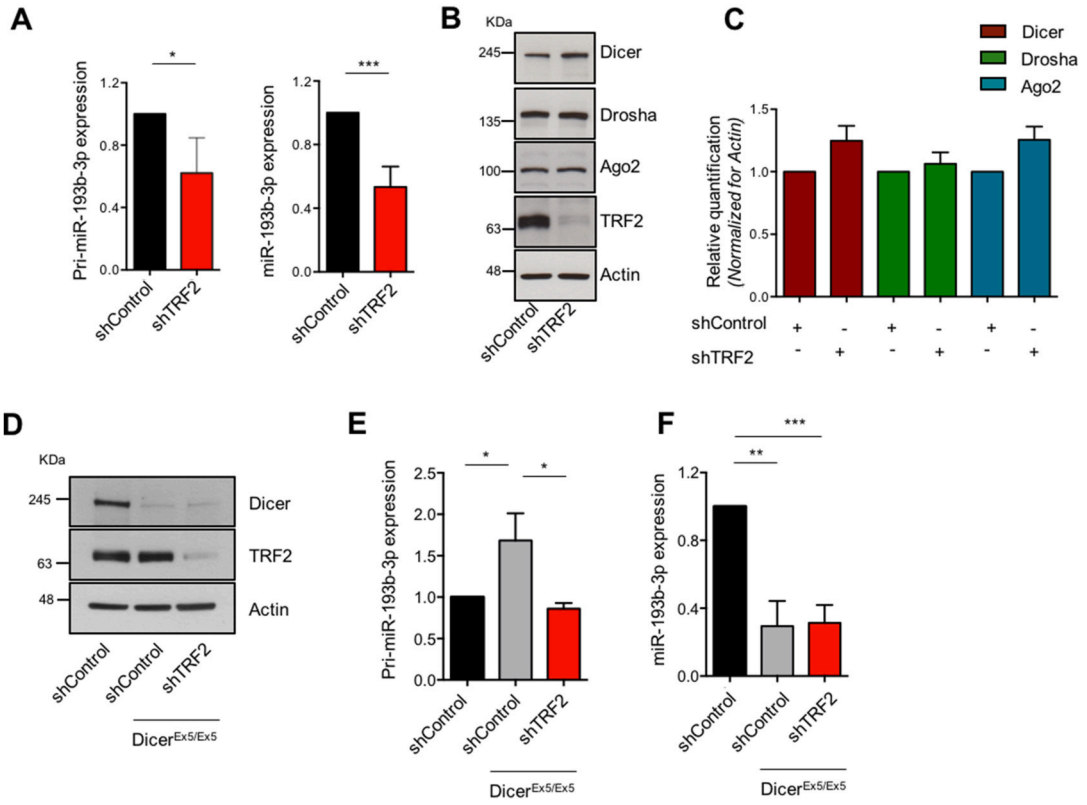

Fig. 2. Modulation of miR-193b-3p by TRF2 is independent from the miRNA biogenesis machinery. (A) Histograms showing the expression levels of pri-miR-193b-3p (left panel) and miR-193b-3p (right panel), evaluated in nuclear and total RNA extracts, respectively, obtained from TRF2-compromised (shTRF2_N1) HCT116 cells and their control counterpart (shControl). Expression levels of miRNA and pri-miRNA were normalized to RNU44 and 18S, respectively. (B) Expression levels of the major components of miRNA biogenesis machinery (Dicer, Drosha, Ago2) were evaluated by western blotting in TRF2 silenced HCT116 cells (shTRF2) and their control counterpart (shControl). TRF2 and Actin were used as internal controls. (C) Quantitative analysis of the western blots shown in (B). Bands' intensity was analysed by Image J software and normalized to actin. (D) Western Blotting showing the expression levels of TRF2 and Dicer evaluated in Dicer-deficient HCT116 cells ($Dicer^{Ex5/Ex5}$), stably silenced for TRF2 (shTRF2) or its control counterpart (shControl). Parental HCT116 cells infected with the control vector (shControl) were used as internal control. Actin levels were evaluated as loading control. (E–F) pri-miR-193b-3p (E) and miR-193b-3p (F) expression levels were evaluated in HCT116 $Dicer^{Ex5/Ex5}$ cells, stably silenced for TRF2 (shTRF2) or its control counterpart (shControl). All the histograms show the mean (±SD) of at least three independent experiments performed in triplicate. P-values (*P < 0.1, **P < 0.01, ***P < 0.001; Student's t-test) are shown. Western blot images are representative of at least three independent experiments.

modulated according to both tests were selected. Statistical significance was set to 5%. A false discovery procedure was included for multiple comparisons.

Unsupervised hierarchical clustering was performed to individuate specific pattern of expression using the Euclidean distance metric.

2.12. Bioinformatic analyses

- Normalized The Cancer Genome Atlas (TCGA) COADREAD gene expression and miRNA expression of tumor samples were obtained from Broad Institute TCGA Genome Data Analysis Center (http://gdac.broadinstitute.org/): Firehose stddata_2016_01_28. Broad Institute of MIT and Harvard (https://doi.org/10.7908/C11G0KM9).

Significance of miRNA and gene modulation between different subgroup of samples was assessed by two-sided Wilcoxon rank sum test. Significance was defined at the $p < 0.05$ level.

Disease-free survival (DFS) and overall survival (OS) were evaluated by using the Kaplan-Meier method and the log-rank test was used to assess differences between curves. A multivariate Cox proportional-hazards regression model was built to evaluate the effect of clinical variables on survival analysis. Patients with high and low signal intensity were defined by considering positive and negative z-score values, if not differently specified. The analyses were completely conducted with Matlab R2020b.

- miRWalk 3.0 web tool (http://mirwalk.umm.uni-heidelberg.de/) was used for miRNA-target interaction prediction.
- Integrative Genomics Viewer (IGV v.2.9.4) was used to visually inspect HCT-116 ChIP-Seq data from the ENCODE project on genome build hg19. The bigWig files, automatically generated by ENCODE uniform processing pipelines in order to facilitate the comparison across datasets, were used for displaying ChIP-Seq data. The following profiles were visualized: GSM1385712 (PolII), GSM1385716 (siTOP1), GSM1385715 (wt_TOP1), GSM3190501 (H3K4me1), GSM3190502 (H3K4me3), GSM3190503 (H3K9ac), GSM3190504 (H3K27ac), GSM3190505 (H3K27me3), GSM3190506 (H3K36me3), GSM3190507 (CTCF).

2.13. Statistical analysis

Statistical analyses, where not specified, were calculated using unpaired t-tests on GraphPad Prism 6. P-values were indicated as followed *P ≤ 0.05; **P ≤ 0.01; ***P ≤ 0.001.

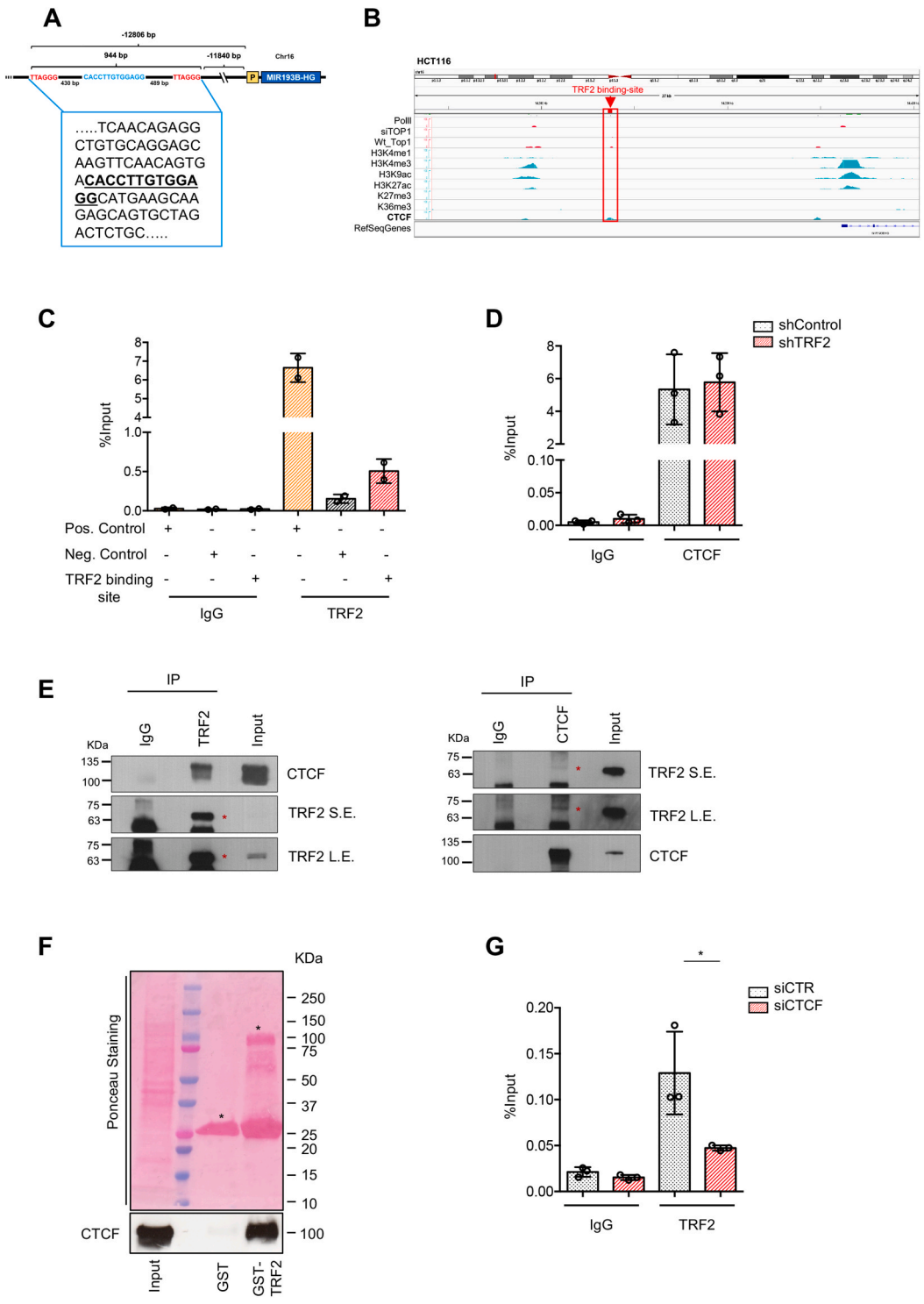

Fig. 3. TRF2 and CTCF interplay is required for miR-193b-3p expression. (A) Schematic representation of DNA region located upstream the miR-193B host gene and containing the putative binding sites for TRF2 and CTCF. (B) Encode data analysis of the DNA portion region around the region identified in (A) was performed in HCT116 cells. The peak of CTCF in correspondence of the putative TRF2 binding-site is evidenced in red. (C) ChIP-qPCR confirming the binding of TRF2 to the motif identified in (A). Histogram shows the mean of two independent experiments. DNA regions containing (Chr.1 sub-telomeric region) or not TTAGGG sequences were used as positive and negative control, respectively. IgGs were used as negative control. (D) Real-time qPCR analysis of TRF2-chromatin immunoprecipitates obtained from HCT116 cells stably silenced for TRF2 (shTRF2) and their control counterpart (shControl). IgGs were used as negative control. (E) Analysis of the interaction between TRF2 and CTCF performed in HCT116 cells. Immunoprecipitations (IP) were performed using an anti-TRF2 (left panel) or anti-CTCF (right panel) antibody and IP products were assayed using anti-CTCF and anti-TRF2 antibodies (S.E. short exposure; L.E. long exposure), respectively. (F) GST pull-down assay of cell lysate from HCT116 cells. Upper panel: Ponceau staining of the GST- or GST-TRF2 (indicated by the asterisks) bound beads. Input corresponds to 5% of the total cell lysate for pull-down. Lower panel: immunoblotting of pull-down products with the anti-CTCF antibody. (G) Real-time qPCR analysis of TRF2-chromatin immunoprecipitates obtained from HCT116 cells silenced for CTCF (siCTCF) and their control counterpart (siControl). IgGs were used as negative control All the histograms show the mean ± SD of at least three independent experiments performed in triplicate (*$P < 0.1$, **$P < 0.01$, ***$P < 0.001$; Student's *t*-test).

3. Results

3.1. TRF2 affects microRNAs expression in CRC cells

In our previous studies, we demonstrated that TRF2 can exert extratelomeric functions through its ability to affect gene expression [7,8,10,12]. Here, we investigated the capability of TRF2 to regulate miRNA expression. To validate this hypothesis, we performed a microarray hybridization assay on HCT116 human colorectal adenocarcinoma cells, stably silenced for TRF2. To this end, cells were transduced with lentiviral particles delivering short-hairpin (sh)RNAs directed against either TRF2 (shTRF2) or a control scramble sequence (shCTRL) and, upon validation of TRF2 silencing (Fig. 1A and Supplementary Fig. 1A), cells underwent RNA extraction and miRNA expression analysis. Interestingly, unsupervised hierarchical clustering analysis, performed on a panel of 2006 miRNAs, identified 162 miRNAs expressed in the evaluated cells (Supplementary Table 2). In particular, ten of the identified miRNAs appeared differentially expressed (4 down-regulated and 6 upregulated) in TRF2-silenced HCT116 cells (shTRF2) compared with their control counterpart (Fig. 1B).

On the basis of their oncogenic or oncosuppressive role in CRC, five of the identified miRNAs (miR-181a-5p, miR-193b-3p, let7i-5p, mir-34a-5p, miR-22–3p), were selected and validated by Taq-Man polymerase chain reaction (Taq-Man qPCR). As reported in Fig. 1C, results of Taq-Man qPCR fully matched with those of the microarray, confirming that TRF2 can control miRNAs expression.

The relationship between TRF2 and the expression of the selected miRNAs was evaluated in a cohort of 621 CRC patients from the TCGA dataset. Clinical data evidenced that miR-193b-3p is the only miRNA, among those evaluated, that correlates in a statistically significant manner ($p = 0.004$) with the levels of TRF2 expression in CRC patients (Fig. 1D–H).

Following the analysis of clinical data, we deeply investigated the molecular link between TRF2 and the expression of miR-193b-3p. To this aim, the levels of the miR-193b-3p were first evaluated in HCT116 cells in which TRF2 expression was modulated either negatively, by chronic infection of a different shRNA (shTRF2_N2, Supplementary Fig. 1B), or positively, by infection with viral particles delivering a cDNA for TRF2 (pBabe-TRF2 Supplementary Fig. 1B). As demonstrated by Taq-Man qPCR, stable overexpression of TRF2 – conversely to its silencing – induced a significant increase of cellular miR-193b-3p levels (Supplementary Fig. 1C). Finally, the capability of TRF2 to regulate the expression of miR-193b-3p was also evaluated in two others CRC cell lines, SW620 and HT29, expressing relatively high and low levels of TRF2, respectively (Supplementary Fig. 1D). To this aim TRF2 was chronically silenced in SW620 (Supplementary Fig. 1E) and overexpressed in HT29 (Supplementary Fig. 1F) and the miR-193b-3p expression was evaluated (Supplementary Figs. 1E–F). Results of Taq Man qPCR evidenced that levels of miR-193b-3p can be affected by modulating TRF2 expression.

3.2. TRF2 and CTCF share DNA binding site and cooperate to promote miR-193b-3p expression

Next, we investigated the molecular mechanism(s) through which TRF2 affects miR-193b-3p expression in tumor cells. In order to address this point, we first evaluated whether TRF2 takes part in the miRNA maturation, a process that, starting from the nascent transcript (the so called pri-miRNA), leads to the synthesis of the mature ~22 nt miRNA. To this aim, HCT116 cells were stably silenced for TRF2 and, upon RNA extraction, the levels of the pri-miRNA and mature miRNA were quantified by Taq-Man qPCR. As reported in the Fig. 2A, silencing of TRF2 induces a similar reduction of both the pri-miRNA and the mature form of miR-193b-3p (about 50% of inhibition). These data were reinforced by Western blot analyses demonstrating that TRF2 does not affect the expression of the main RISC complex components (*i.e.* Drosha, Dicer and Ago2) (Fig. 2B–C), indicating that TRF2 regulates the levels of miR-193b-3p without affecting the maturation machinery. Moreover, experiments performed in Dicer-deficient cells (HCT116 Dicer$^{ex5/ex5}$ [31], Fig. 2D), demonstrated that impairment of the maturation machinery determines an accumulation of the immature miR-193b-3p at the expenses of its mature form (Fig. 2E–F). Under these conditions, silencing of TRF2 (Fig. 2D) – even maintaining the capability of impairing the pri-miRNA levels (Fig. 2E) – does not produce additive effects on the mature miRNA (Fig. 2F), suggesting that TRF2 is acting upstream the miRNA maturation, possibly by affecting the transcription process.

Knowing that TRF2 can regulate gene expression through its binding to proximal (promoters) or distal (enhancers) regulatory elements of the DNA [6–12], we analysed a region of about 20 Kb upstream the transcription starting site (TSS) of the miR-193b-3p host-gene (hg38-Chr16:14,302,288–14,331,067), looking for putative TRF2 binding sites. As reported in Fig. 3A, the bioinformatic search identified a putative binding region for TRF2 – containing two ITS (TTAGGG) – in the position ranging from 14,289,483 to 14,290,427 of the chromosome 16. To understand if the identified region would fall into a transcriptionally active portion of the DNA, the state of the chromatin around the putative binding sites of TRF2 was evaluated in a panel of ChIP-Seq data on HCT116 cells, available within the ENCODE project. As schematically reported in Fig. 3B, the analysis of the ENCODE data did not evidence, in the proximity of the evaluated region, any enrichment of markers (*e.g.* PolII, Top 1, histones' modifications) typically associated with gene promoters and/or enhancers [32,33] suggesting that the control of miR-193b-3p expression by TRF2 is reasonably due to other regulatory mechanisms.

Even if extratelomeric functions of TRF2 are now well-recognised, the mechanisms through which this protein affects gene expression are still not completely elucidated. Interestingly, quite recent studies evidenced an enrichment of the chromatin organization factor CTCF in DNA regions proximal to the binding sites of TRF2, suggesting that TRF2 and CTCF might work cooperatively [34,35]. In accordance with these data, *in-silico* analyses performed with LASAGNA-search 2.0, a web tool for transcription factor binding site search, identified a putative binding site for CTCF (CAGTGACACCTTGTGGAGGCA), which is localized upstream the host-gene of miR-193b-3p (hg38-Chr16:14,289,913–14,289,934) and contained within the previously identified region of TRF2 binding (Fig. 3A). Starting from this observation – confirmed also by the Encode data analysis (Fig. 3B) – we pointed at elucidating the link existing between TRF2 and CTCF. To this aim, we assessed, first of all, the binding of TRF2 and CTCF to the identified DNA region. Interestingly, ChIP assays demonstrated that TRF2 seats on the same region occupied by CTCF (Fig. 3C–D). Moreover, as shown by immunoprecipitation (IP) experiments and subsequent GST pull-down assay, the two proteins physically interact (Fig. 3E–F). Interestingly, ChIP experiments performed by silencing either TRF2 or CTCF, demonstrated that while knocking-down of TRF2 (Supplementary Fig. 2A) did not affect the binding of CTCF to its target motif (Fig. 3D), the down-regulation of CTCF (Supplementary Fig. 2B) significatively reduced the binding of TRF2 to the DNA (Fig. 3G). These results, together with the data showing that silencing of TRF2 significatively reduces the cellular levels of miR-193b-3p (Figs. 1C and 2A), would indicate that the transcriptional control of the miRNA is dependent on TRF2 while CTCF controls the proper positioning of TRF2 on its DNA binding-motif.

3.3. miR-193b-3p promotes cells growth by targeting SUV39H1

Next we evaluated the role of miR-193b-3p as a possible functional effector of the pro-oncogenic activity of TRF2 in tumor cells. The role of miR-193b-3p is largely debated in the literature. Indeed, while a number of studies have documented tumor suppressive functions of miR-193b-3p [36–40], other reports have attributed to the same miRNA a clear pro-tumoral activity [41–47]. Starting from these considerations, we decided to evaluate the effect of miR-193b-3p on cell growth in our CRC

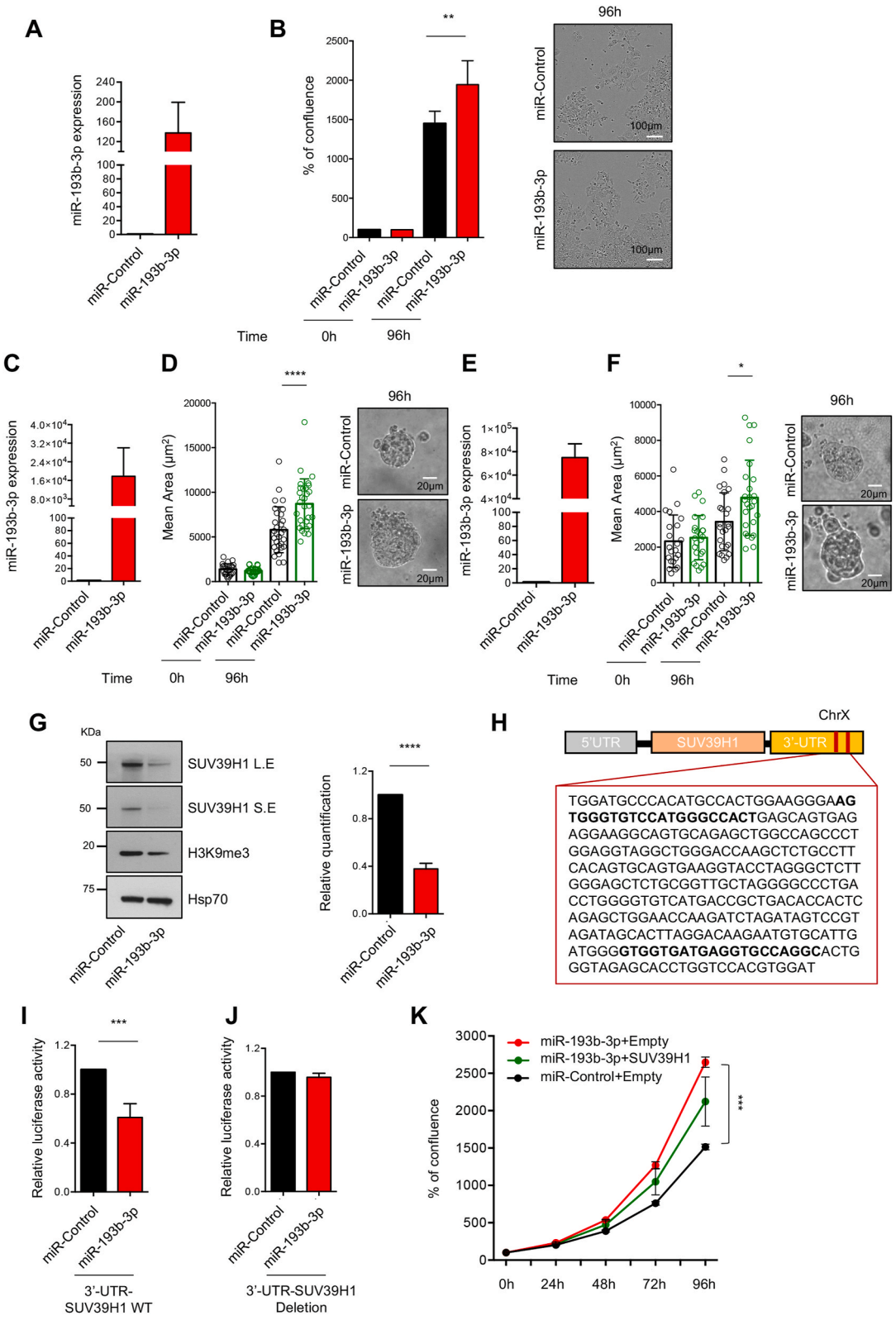

(caption on next page)

Fig. 4. miR-193b-3p promotes colon cancer proliferation by targeting SUV39H1. (A) TaqMan qPCR analysis of miR-193b-3p levels in HCT116 cells 72h after transfection of miR193b3p or its control counterpart (miR-Control). (B) Proliferation of HCT116 cells over-expressing miR-193b-3p, and their control counterpart (miR-Control), was monitored by time-lapse imaging by Incucyte analysis. Left panel: percentage of cell confluence at time 0 and 96 h. Histogram shows the mean (±SE) of four independent experiments performed in quadruplicates. Statistical analysis was performed by paired *t*-test. Right panel: representative images showing the cell confluence at the final point of the time course analysis (96 h). (C–F) Ectopic expression of miR-193b-3p in two different organoids was evaluated by TaqMan qPCR (C and E). At least 20 organoids of CRC #0327 (D) and #0125 (F) were taken at the indicated times using the Leica DMi8 (magnification 20×). The area of each organoid was measured by Image J software. Representative image of each sample (right panel D and F) at 96h is shown. Histograms show the mean ± SD of two independent experiments. (G) Expression levels of SUV39H1 and H3K9me3 were evaluated by western blotting in HCT116 72h after the transfection with miR-193b-3p, or its control counterpart (miR-Control). Left panel: representative images showing the expression levels of SUV39H1 (S.E. short exposure; L.E. long exposure) and H3K9me3. HSP70 was used as loading control. Right panel: quantitative analysis of the western blots. Bands' intensity was analysed by Image J software and normalized to HSP70 (H) Scheme showing the sequences (in bold) of two putative binding sites of miR-193b-3p in the 3′UTR of SUV39H1. (I–J) Binding specificity of miR193b-3p on the 3′UTR of SUV39H1 was evaluated by luciferase assay. The wild type (I) and the mutated (J) forms of 3′UTR of SUV39H1, cloned into the dual-luciferase reporter vector psiCHECK-2, were co-transfected with the miR-193b-3p in HCT116 and luciferase activity was assayed. Results are expressed as fold change over the activity measured in the cells transfected with control miRNA. (K) HCT116 cells overexpressing miR-193b-3p were transiently transfected with SUV39H1 and cell proliferation was evaluated by Incucyte. Results shows the percentage of cell confluence at indicated time points. When not specified, histograms show the mean ± SD of at least three independent experiments performed in triplicate (*$P < 0.1$, **$P < 0.01$, ***$P < 0.001$; Student's *t*-test).

models. Interestingly, we found that either over-expression of miR-193b-3p or TRF2 (Fig. 4A and Supplementary Fig. 2C), significantly increased cell proliferation (Fig. 4B and Supplementary Fig. 2D), while silencing of TRF2 reduced cell growth and this effect was reverted by miR-193b-3p over-expression (Supplementary Fig. 2E), demonstrating the role of this miRNA as a functional effector of TRF2 activity.

To reinforce our findings, we moved from simple bi-dimensional cell models to more advanced *in vitro* models. In particular, experiments were performed on human organoids – three-dimensional structures obtained from CRC patients' cells, which maintain the structural and functional complexity of the tumor of origin. Interestingly, time-lapse microscopy experiments evidenced that miR-193b-3p overexpression (Fig. 4C and E) was able to significantly favour the growth of two different organoids (CRC-0327 and CRC-0125), thus confirming the oncogenic role of miR-193b-3p (Fig. 4D and F).

Next, with the aim of identifying the targets of the miR-193b-3p, we performed a bioinformatic analysis by miRWalk 3.0, an open-source prediction software. Among the most promising targets identified (binding-p > 0.8, Supplementary Table 3), we focused on suppressor of variegation 3–9 homolog 1 (SUV39H1), a histone methyltransferase that, by trimethylating lysine-9 of histone H3 (H3K9-3me), regulates DNA hetero-chromatinization and participates, like TRF2, in maintenance of telomere stability [48–51]. To validate the results of the *in-silico* analysis, the capability of miR-193b-3p to target SUV39H1 was evaluated in HCT116 cells. Notably, Western blot analysis evidenced that SUV39H1 levels (Fig. 4G) – as well as those of its downstream effector, the histone H3 lysine-9 trimethylated (H3K9me3, Fig. 4G) – significantly decreased in miRNA over-expressing cells. Conversely, depletion of either TRF2 or CTCF promoted the expression of SUV39H1 and H3K9me3 (Supplementary Fig. 2F), confirming that both TRF2 and CTCF take part in the control of miR-193b-3p expression.

Next, we investigated the mechanism(s) through which miR-193b-3p affects SUV39H1 expression. Notably, the mRNA of SUV39H1– evaluated by RT-PCR – was not affected by miRNA over-expression (Supplementary Fig. 2G), indicating that miR-193b-3p is not acting at the transcriptional level.

Predictive analysis recognizes, for each target, the regions (5′-UTR/CDS/3′UTR) that are putatively targeted by miRNAs. Concerning our analysis, the software identified, in the 3′-UTR of SUV39H1, two putative binding sequences for miR-193b-3p (Fig. 4H and Supplementary Table 4). Starting from these data, we extended our analysis by performing a luciferase assay aimed at definitively validating SUV39H1 as a target of miR-193b-3p. In detail, a portion of about 2000 bp of the 3′-UTR of SUV39H1containing the two binding sites for the miR-193b-3p (Fig. 4H and Supplementary Table 4), was cloned into a dual-luciferase reporter vector (psiCHECK-2), downstream the Renilla coding gene, and the effect of the miRNA was evaluated in the cells upon co-transfection of this reporter construct with the synthetic mimic-miR-193b-3p or its control counterpart (miR-CTRL). As reported in Fig. 4I, the over-expression of miR-193b-3p significantly impaired the expression of Renilla. To prove that the effect of the miRNA was really due to its capability of targeting the 3′UTR of SUV39H1, the two binding-sites were then mutagenized and the effect of miR-193b-3p was evaluated. Interestingly, deletion of both binding-sites completely abolished the effect of the miRNA, indicating that each of the two sites is sufficient for promoting miRNA binding and activity (Fig. 4J).

As reported in the literature, forced expression of SUV39H1 exerts a growth-suppressive and transcriptional repressive role [52], which results in increased tumor protection in transgenic mice models [30]. Since the tumor-suppressive properties of SUV39H1 inversely correlate with those of miR-193b-3p, we pointed at clarifying the role of the miR-193b-3p/SUV39H1 axis on tumor cell proliferation. Interestingly, cell growth analyses – performed in HCT116 cells over-expressing or not miR-193b-3p – demonstrated that ectopic expression of SUV39H1 (Supplementary Fig. 2H) counteracted the proliferative activity of the miRNA (Fig. 4K), confirming that pro-tumoral activity of miR-193b-3p goes mainly through its capability of targeting SUV39H1.

3.4. *miR-193b-3p and TRF2 have a prognostic impact on survival of CRC patients*

Finally, the clinical-pathological relevance of our findings was evaluated in a cohort of 621 CRC patients from the TCGA dataset. Notably, our analyses evidenced that miR-193b-3p expression positively correlates with tumor stage, lymph-node positivity and tumor metastasis. Indeed, stage III and IV CRC patients, and particularly those with lymph-nodal (N+) and/or distal (M+) metastases, were found to be associated with higher levels of miR-193b-3p (Fig. 5A–C). These data, fitting with those obtained by evaluating the levels of TRF2 in the same cohort of patients (Fig. 5D–F), sustained and reinforced the idea that a number of the oncogenic activities driven by TRF2 in CRC are mediated by miR-193b-3p. Moreover, analysis of patients' survival evidenced that those subjects expressing high levels of both TRF2 and miR-193b-3p (miR-193^{high}/TRF2^{high}, $Z_{score}>0$) have a worst prognosis than the patients expressing low levels of the two variables (miR-193b^{low}/TRF2^{low}, $Z_{score}<0$; Fig. 5G). These results, confirmed also excluding the patients at stage I and IV (two patients' sub-populations with a well-predictable clinical outcome; Fig. 5H), attributed a prognostic value to TRF2/miR-193b-3p association.

4. Discussion

In recent years, the extratelomeric properties of TRF2 have been the focus of numerous studies. Indeed, it is now clear that TRF2, through its capability to bind DNA sequences located outside telomeres, affects the expression of a number of genes involved in tumor formation and progression [6–12]. In this context, our recent findings contributed to identify a number of TRF2-target genes able to affect either the

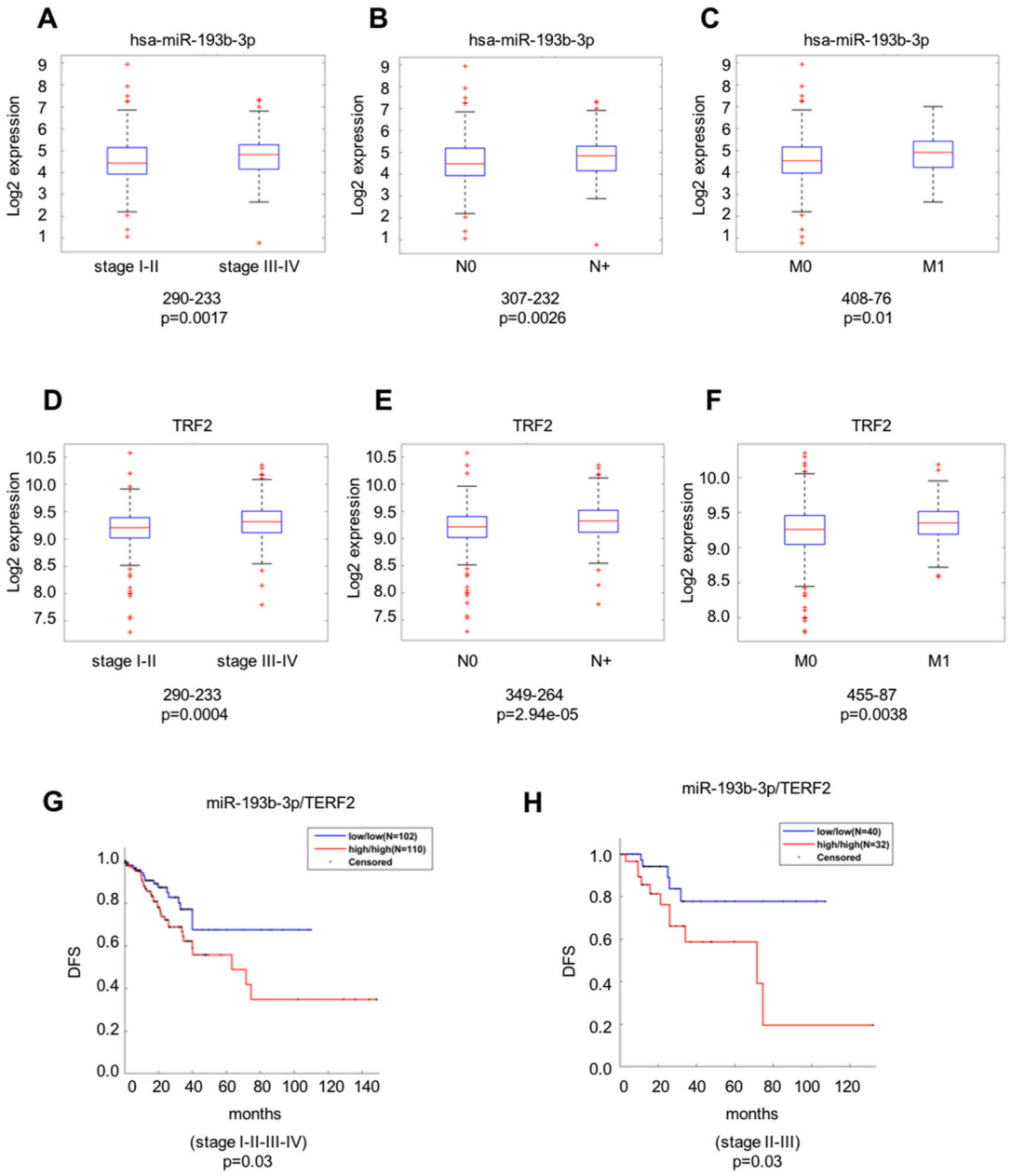

Fig. 5. Positive correlation between TRF2 and miR193b-3p has a prognostic impact on patients' survival. (A–F) Evaluation of miR-193b-3p and TRF2 expression levels in a cohort of CRC patients from the TCGA dataset. Analyses were performed on the CRC patients categorized on the basis of three parameters: (A and D) tumor stage (I-II vs III-IV), (B and E) lymph-node positivity (N0 vs N+) and (C and F) presence of distal metastases (M0. vs M1). On each box, the central mark is the median, the edges of the box are the 25th and 75th percentiles and the outliers are plotted individually. (G–H) Analysis of survival performed on a cohort of CRC patients stratified on the basis of miR-193b-3p/TRF2 expression levels (high/high vs low/low). The Disease-free survival (DFS) evaluated by Kaplan-Meir curves was performed by either including all tumor stages (G) or only the stages II-III (H). Statistical significance between distributions of subgroups of patients was assessed by two-sided Wilcoxon rank sum test. The number of CRC patients (N) and the p-values are directly reported in the figure.

recruitment and the activation of MDSC and NK – with a consequent impact on tumor immune-escape [7,10] – as well as the extracellular release of VEGF-A and tumor angiogenesis [12].

Here we did a step forward by demonstrating that TRF2, in addition to genes, also regulates miRNAs, small non coding RNA that, acting at the post-transcriptional level, are able to directly affect protein expression. Among the miRNAs found regulated by TRF2 in CRC, we focused on miR-193b-3p, a miRNA that positively correlates with TRF2 expression in human patients.

The role of miR-193b-3p in cancer is quite debated and still controversial. Indeed, while a number of studies emphasized the tumor-suppressive activity of this miRNA in different tumor types and cell lines [36–40], several others conversely demonstrated that miR-193b-3p functions as an oncogene and reported its overexpression in a number of tumors, including CRC, in which this miRNA plays a key role in tumor progression [41–47]. Despite the apparent incongruences among the different studies, a more detailed analysis of the data available in the literature seems to suggest that the behaviour of miR-193b-3p is dependent on tumor type.

In the present work, we started by evaluating the impact of the over-expression of miR-193b-3p in terms of tumor growth. In all the CRC models that we tested, both simple bidimensional cell cultures and also human organoids derived from patients, over-expression of the miRNA exerts a positive impact on tumor proliferation, indicating that this

miRNA is a downstream effector of the tumor-intrinsic promoting activities of TRF2.

Since the information concerning the target of miR-193b-3p are still very poor, we next pointed at identifying the target of the miRNA that would explain its pro-tumoral activity. Using a bioinformatic predictive tool, we searched for the targets of the miR-193b-3p, identifying – as expected – thousands of putative target genes. Next, based on the data available in the literature and taking into account the link between the evaluated targets and the functional roles associated with TRF2 expression, we narrowed up to focus on, SUV39H1, a histone methyltransferase with an already known role as tumor-suppressor. Notably, identifying this target of miR-193b-3p, and demonstrating that its overexpression is able to revert the effect of miR-193b-3p on tumor growth, we defined at least one of the cell-intrinsic pathways through which TRF2 exerts it tumor promoting activity.

Subsequently, we explored the mechanism(s) through which TRF2 affects miRNA expression. Notably, our data demonstrated that TRF2 does not take part in the miRNA maturation process, evidencing – conversely – the capability of TRF2 to exert its control activity by acting at the transcriptional level. Results of bioinformatic analyses, followed by experimental validation, demonstrated that control of transcription by TRF2 depends on its binding to telomere-like sequences located upstream the miR-193b-3p host gene. Different from our previous studies demonstrating that the control of gene expression by TRF2 was dependent on its binding to gene-regulatory elements (promoters or enhancers) [7,10,12], here we found that the binding-site of TRF2 falls into a region distant from the promoter of miR-193b-3p host-gene and missing the typical characteristics of the enhancers, finally suggesting that transcriptional control of the miRNA would be dependent on a different mechanism of TRF2 action. Notably, we demonstrated that CTCF, a chromatin organization factor involved in regulation of gene expression, binds a region of DNA very close to the binding-site of TRF2, suggesting that this factor could take part in the mechanism of transcriptional control exerted by TRF2 on miR-193b-3p expression. The mechanism through which CTCF takes part in control of gene expression has been long studied in the literature. This zinc-finger protein that was originally identified in a context of gene silencing and repression [53,54], was subsequently shown to be involved in a large array of transcriptional mechanisms, including gene activation [55], insulation [56–59], imprinting [60–62] and X chromosome inactivation [63–65]. Notably, these multiple (and sometimes diametrically opposed) regulatory activities of CTCF have been found to not directly depend on its transcriptional activity but rather on the capability of this protein to affect the global organization of chromatin architecture. Indeed, the DNA binding of CTCF mediates the formation of inter- and intra-chromosomal loops that, putting in contact distant regions of the genome, would permit the control of gene transcription by its DNA-binding partners [66–68].

In line with these data, we found that CTCF interacts with TRF2 and it drives the proper positioning of TRF2 on its binding site on the DNA. However, TRF2 is the factor really involved in the transcription of miR-193b-3p; indeed, silencing of TRF2 impairs miRNA expression without affecting the DNA binding of CTCF. Here, although we do not provide a direct demonstration of the capability of CTCF to promotes DNA bending (an aspect that will be the tackled in future studies), we defined a novel and previously unreported mechanism through which TRF2 can regulate transcription of miRNAs and/or genes, thus defining a general process that would be at the root of the wide variety of extratelomeric functions exerted by TRF2.

Finally, we also evaluated the clinical-pathological relevance of our findings by assessing the prognostic role of the positive association between TRF2 and the miR-193b-3p in a cohort of CRC patients. Since prediction of clinical outcome of CRC patients is currently based mainly on the evaluation of tumor stage, lymph-node positivity and presence of distant metastases [69], we first evaluated the existence of a correlation between these parameters and the levels of miR-193b-3p and TRF2. Interestingly, our analyses evidenced that both TRF2 and miR-193b-3p are more expressed in stage II and III patients with positive lymph-nodes and distal metastases, and TRF2/miR-193b-3p association negatively impacts on the clinical outcome of the evaluated subjects, opening the way towards a possible clinical application of our results.

Overall, these data expand our general knowledge about cancer-related activities of TRF2. Further, the results presented here put forward the prognostic value of TRF2/miR-193b-3p association as a biomarker that could be deployed for predicting the clinical outcome of those patients (especially stage II and III) with an uncertain clinical fate.

Fundings

This work was financially supported by Ministry of Health [intramural grant-in-aid to P.Z. and M.P.] and by Italian Association for Cancer Research [21579 to A.B.]. R.D. and E.P. were recipients of a fellowship from the Italian Foundation for Cancer Research (FIRC).

Author contributions

Conception and design: R. Dinami, P. Zizza and A. Biroccio. Acquisition of data: E. Petti, A. Rizzo, M. Porru, F.Ganci. Analysis and interpretation of data: E. Petti, M. Porru, P. Ostano, A. Sacconi. Data curation: R. Dinami, P. Zizza and A. Biroccio. Supervision: G. Chiorino, L. Trusolino, G. Blandino, G. Ciliberto, P. Zizza, A. Biroccio. Writing original draft: P. Zizza and A. Biroccio. Funding Acquisition: M. Porru, P. Zizza, A. Biroccio.

Declaration of interests

The authors declare that they have no known competing financial interests or personal relationships that could have appeared to influence the work reported in this paper.

Acknowledgements

The authors would like to thank professor Bert Vogelstein (Johns Hopkins University, Baltimore, MD, USA), professor Eric Gilson (IRCAN, Nice, France), professor Michele Milella (University of Verona, Verona, Italy) and professor Stefan Shoeftner (University of Trieste, Trieste, Italy) for providing cell lines and constructs.

Appendix A. Supplementary data

Supplementary data to this article can be found online at https://doi.org/10.1016/j.canlet.2022.215607.

References

[1] W. Palm, T. de Lange, How shelterin protects mammalian telomeres, Annu. Rev. Genet. 42 (2008) 301–334, https://doi.org/10.1146/annurev.genet.41.110306.130350.

[2] S. Feuerhahn, L. yow Chen, B. Luke, A. Porro, No DDRama at chromosome ends: TRF2 takes centre stage, Trends Biochem. Sci. 40 (2015) 275–285, https://doi.org/10.1016/j.tibs.2015.03.003.

[3] D. Benarroch-Popivker, S. Pisano, A. Mendez-Bermudez, L. Lototska, P. Kaur, S. Bauwens, N. Djerbi, C.M. Latrick, V. Fraisier, B. Pei, A. Gay, E. Jaune, K. Foucher, J. Cherfils-Vicini, E. Aeby, S. Miron, A. Londoño-Vallejo, J. Ye, M.H. le Du, H. Wang, E. Gilson, M.J. Giraud-Panis, TRF2-Mediated control of telomere DNA topology as a mechanism for chromosome-end protection, Mol. Cell 61 (2016) 274–286, https://doi.org/10.1016/j.molcel.2015.12.009.

[4] T. Simonet, L.E. Zaragosi, C. Philippe, K. Lebrigand, C. Schouteden, A. Augereau, S. Bauwens, J. Ye, M. Santagostino, E. Giulotto, F. Magdinier, B. Horard, P. Barbry, R. Waldmann, E. Gilson, The human TTAGGG repeat factors 1 and 2 bind to a subset of interstitial telomeric sequences and satellite repeats, Cell Res. 21 (2011) 1028–1038, https://doi.org/10.1038/cr.2011.40.

[5] A. Mendez-Bermudez, L. Lototska, S. Bauwens, M.J. Giraud-Panis, O. Croce, K. Jamet, A. Irizar, M. Mowinckel, S. Koundrioukoff, N. Nottet, G. Almouzni, M. P. Teulade-Fichou, M. Schertzer, M. Perderiset, A. Londoño-Vallejo, M. Debatisse, E. Gilson, J. Ye, Genome-wide control of heterochromatin replication by the

telomere capping protein TRF2, Mol. Cell 70 (2018) 449–461, https://doi.org/10.1016/j.molcel.2018.03.036, e5.
[6] D. Yang, Y. Xiong, H. Kim, Q. He, Y. Li, R. Chen, Z. Songyang, Human telomeric proteins occupy selective interstitial sites, Cell Res. 21 (2011) 1013–1027, https://doi.org/10.1038/cr.2011.39.
[7] A. Biroccio, J. Cherfils-Vicini, A. Augereau, S. Pinte, S. Bauwens, J. Ye, T. Simonet, B. Horard, K. Jamet, L. Cervera, A. Mendez-Bermudez, D. Poncet, R. Grataroli, C.T. K. de Rodenbeeke, E. Salvati, A. Rizzo, P. Zizza, M. Ricoul, C. Cognet, T. Kuilman, H. Duret, F. Lépinasse, J. Marvel, E. Verhoeyen, F.L. Cosset, D. Peeper, M.J. Smyth, A. Londoño-Vallejo, L. Sabatier, V. Picco, G. Pages, J.Y. Scoazec, A. Stoppacciaro, C. Leonetti, E. Vivier, E. Gilson, TRF2 inhibits a cell-extrinsic pathway through which natural killer cells eliminate cancer cells, Nat. Cell Biol. 15 (2013) 818–828, https://doi.org/10.1038/ncb2774.
[8] J. Ye, V.M. Renault, K. Jamet, E. Gilson, Transcriptional outcome of telomere signalling, Nat. Rev. Genet. 15 (2014) 491–503, https://doi.org/10.1038/nrg3743.
[9] T. Hussain, D. Saha, G. Purohit, A. Kar, A. Kishore Mukherjee, S. Sharma, S. Sengupta, P. Dhapola, B. Maji, S. Vedagopuram, N.T. Horikoshi, N. Horikoshi, R. K. Pandita, S. Bhattacharya, A. Bajaj, J.F. Riou, T.K. Pandita, S. Chowdhury, Transcription regulation of CDKN1A (p21/CIP1/WAF1) by TRF2 is epigenetically controlled through the REST repressor complex, Sci. Rep. 7 (2017), https://doi.org/10.1038/s41598-017-11177-1.
[10] J. Cherfils-Vicini, C. Iltis, L. Cervera, S. Pisano, O. Croce, N. Sadouni, B. Győrffy, R. Collet, V.M. Renault, M. Rey-Millet, C. Leonetti, P. Zizza, F. Allain, F. Ghiringhelli, N. Soubeiran, M. Shkreli, E. Vivier, A. Biroccio, E. Gilson, Cancer cells induce immune escape via glycocalyx changes controlled by the telomeric protein TRF 2, EMBO J. 38 (2019), https://doi.org/10.15252/embj.2018100012.
[11] A.K. Mukherjee, S. Sharma, S. Bagri, R. Kutum, P. Kumar, A. Hussain, P. Singh, D. Saha, A. Kar, D. Dash, S. Chowdhury, Telomere repeat-binding factor 2 binds extensively to extra-telomeric G-quadruplexes and regulates the epigenetic status of several gene promoters, J. Biol. Chem. 294 (2019) 17709–17722, https://doi.org/10.1074/jbc.RA119.008687.
[12] P. Zizza, R. Dinami, M. Porru, C. Cingolani, E. Salvati, A. Rizzo, C. D'Angelo, E. Petti, C.A. Amoreo, M. Mottolese, I. Sperduti, A. Chambery, R. Russo, P. Ostano, G. Chiorino, G. Blandino, A. Sacconi, J. Cherfils-Vicini, C. Leonetti, E. Gilson, A. Biroccio, TRF2 positively regulates SULF2 expression increasing VEGF - a release and activity in tumor microenvironment, Nucleic Acids Res. 47 (2019) 3365–3382, https://doi.org/10.1093/nar/gkz041.
[13] K. Nakanishi, T. Kawai, F. Kumaki, S. Hiroi, M. Mukai, E. Ikeda, C.E. Koering, E. Gilson, Expression of mRNAs for telomeric repeat binding factor (TRF)-1 and TRF2 in atypical adenomatous hyperplasia and adenocarcinoma of the lung, Clin. Cancer Res. 9 (2003) 1105–1111. http://clincancerres.aacrjournals.org/content/9/3/1105.abstract.
[14] M.C. Diehl, M.O. Idowu, K.N. Kimmelshue, T.P. York, C.K. Jackson-Cook, K. C. Turner, S.E. Holt, L.W. Elmore, Elevated TRF2 in advanced breast cancers with short telomeres, Breast Cancer Res. Treat. 127 (2011) 623–630, https://doi.org/10.1007/s10549-010-0988-7.
[15] M. el Maï, K.D. Wagner, J.F. Michiels, D. Ambrosetti, A. Borderie, S. Destree, V. Renault, N. Djerbi, M.J. Giraud-Panis, E. Gilson, N. Wagner, The telomeric protein TRF2 regulates angiogenesis by binding and activating the PDGFRβ promoter, Cell Rep. 9 (2014) 1047–1060, https://doi.org/10.1016/j.celrep.2014.09.038.
[16] R. Blanco, P. Muñoz, J.M. Flores, P. Klatt, M.A. Blasco, Telomerase abrogation dramatically accelerates TRF2-induced epithelial carcinogenesis, Gene Dev. 21 (2007) 206–220, https://doi.org/10.1101/gad.406207.
[17] I. Diala, N. Wagner, F. Magdinier, M. Shkreli, M. Sirakov, S. Bauwens, C. Schluth-Bolard, T. Simonet, V.M. Renault, J. Ye, A. Djerbi, P. Pineau, J. Choi, S. Artandi, A. Dejean, M. Plateroti, E. Gilson, Telomere protection and TRF2 expression are enhanced by the canonical Wnt signalling pathway, EMBO Rep. 14 (2013) 356–363, https://doi.org/10.1038/embor.2013.16.
[18] P. Muñoz, R. Blanco, J.M. Flores, M.A. Blasco, XPF nuclease-dependent telomere loss and increased DNA damage in mice overexpressing TRF2 result in premature aging and cancer, Nat. Genet. 37 (2005) 1063–1071, https://doi.org/10.1038/ng1633.
[19] A. Biroccio, A. Rizzo, R. Elli, C.E. Koering, A. Belleville, B. Benassi, C. Leonetti, M. F.G. Stevens, M. D'Incalci, G. Zupi, E. Gilson, TRF2 inhibition triggers apoptosis and reduces tumourigenicity of human melanoma cells, Eur. J. Cancer 42 (2006) 1881–1888, https://doi.org/10.1016/j.ejca.2006.03.010.
[20] Y. Bai, J.D. Lathia, P. Zhang, W. Flavahan, J.N. Rich, M.P. Mattson, Molecular targeting of TRF2 suppresses the growth and tumorigenesis of glioblastoma stem cells, Glia 62 (2014) 1687–1698, https://doi.org/10.1002/glia.22708.
[21] J. Wang, J. Chen, S. Sen, MicroRNA as biomarkers and diagnostics, J. Cell. Physiol. 231 (2016) 25–30, https://doi.org/10.1002/jcp.25056.
[22] B. Zhang, X. Pan, G.P. Cobb, T.A. Anderson, microRNAs as oncogenes and tumor suppressors, Dev. Biol. 302 (2007) 1–12, https://doi.org/10.1016/j.ydbio.2006.08.028.
[23] S.J. Ankasha, M.N. Shafiee, N.A. Wahab, R.A.R. Ali, N.M. Mokhtar, Post-transcriptional regulation of microRNAs in cancer: from prediction to validation, Onco Rev. 12 (2018) 39–44, https://doi.org/10.4081/oncol.2018.344.
[24] C.E. Condrat, D.C. Thompson, M.G. Barbu, O.L. Bugnar, A. Boboc, D. Cretoiu, N. Suciu, S.M. Cretoiu, S.C. Voinea, miRNAs as biomarkers in disease: latest findings regarding their role in diagnosis and prognosis, Cells 9 (2020), https://doi.org/10.3390/cells9020276.
[25] Y. Shi, Z. Liu, Q. Lin, Q. Luo, Y. Cen, J. Li, X. Fang, C. Gong, MiRNAs and cancer: key link in diagnosis and therapy, Genes 12 (2021) 1289, https://doi.org/10.3390/genes12081289.
[26] M.v. Iorio, C.M. Croce, microRNA involvement in human cancer, Carcinogenesis 33 (2012) 1126–1133, https://doi.org/10.1093/carcin/bgs140.
[27] Y. Peng, C.M. Croce, The role of microRNAs in human cancer, Signal Transduction and Targeted Therapy. https://doi.org/10.1038/sigtrans.2015.4, 2016, 1.
[28] M. van de Wetering, H.E. Francies, J.M. Francis, G. Bounova, F. Iorio, A. Pronk, W. van Houdt, J. van Gorp, A. Taylor-Weiner, L. Kester, A. McLaren-Douglas, J. Blokker, S. Jaksani, S. Bartfeld, R. Volckman, P. van Sluis, V.S.W. Li, S. Seepo, C. Sekhar Pedamallu, K. Cibulskis, S.L. Carter, A. McKenna, M.S. Lawrence, L. Lichtenstein, C. Stewart, J. Koster, R. Versteeg, A. van Oudenaarden, J. Saez-Rodriguez, R.G.J. Vries, G. Getz, L. Wessels, M.R. Stratton, U. McDermott, M. Meyerson, M.J. Garnett, H. Clevers, Prospective derivation of a living organoid biobank of colorectal cancer patients, Cell 161 (2015) 933–945, https://doi.org/10.1016/j.cell.2015.03.053.
[29] J. Karlseder, A. Smogorzewska, T. de Lange, Senescence induced by altered telomere state, not telomere loss, Science 295 (2002) 2446–2449, https://doi.org/10.1126/science.1069523.
[30] E. Petti, F. Jordi, V. Buemi, R. Dinami, R. Benetti, M.A. Blasco, S. Schoeftner, Altered telomere homeostasis and resistance to skin carcinogenesis in suv39h1 transgenic mice, Cell Cycle 14 (2015) 1438–1446, https://doi.org/10.1080/15384101.2015.1021517.
[31] J.M. Cummins, Y. He, R.J. Leary, R. Pagliarini, L.A. Diaz, T. Sjoblom, O. Barad, Z. Bentwich, A.E. Szafranska, E. Labourier, C.K. Raymond, B.S. Roberts, H. Juhl, K. W. Kinzler, B. Vogelstein, V.E. Velculescu, The colorectal microRNAome, Proc. Natl. Acad. Sci. U.S.A. 103 (2006) 3687–3692, https://doi.org/10.1073/pnas.0511155103.
[32] E. Calo, J. Wysocka, Modification of enhancer chromatin: what, how, and why? Mol. Cell 49 (2013) 825–837, https://doi.org/10.1016/j.molcel.2013.01.038.
[33] L.A. Gates, C.E. Foulds, B.W. O'Malley, Histone marks in the 'driver's seat': functional roles in steering the transcription cycle, Trends Biochem. Sci. 42 (2017) 977–989, https://doi.org/10.1016/j.tibs.2017.10.004.
[34] Z. Deng, Z. Wang, N. Stong, R. Plasschaert, A. Moczan, H.S. Chen, S. Hu, P. Wikramasinghe, R.v. Davuluri, M.S. Bartolomei, H. Riethman, P.M. Lieberman, A role for CTCF and cohesin in subtelomere chromatin organization, TERRA transcription, and telomere end protection, EMBO J. 31 (2012) 4165–4178, https://doi.org/10.1038/emboj.2012.266.
[35] N. Stong, Z. Deng, R. Gupta, S. Hu, S. Paul, A.K. Weiner, E.E. Eichler, T. Graves, C. C. Fronick, L. Courtney, R.K. Wilson, P.M. Lieberman, R.v. Davuluri, H. Riethman, Subtelomeric CTCF and cohesin binding site organization using improved subtelomere assemblies and a novel annotation pipeline, Genome Res. 24 (2014) 1039–1050, https://doi.org/10.1101/gr.166983.113.
[36] J. Chen, X. Zhang, C. Lentz, M. Abi-Daoud, G.C. Paré, X. Yang, H.E. Feilotter, V. A. Tron, MiR-193b regulates Mcl-1 in melanoma, Am. J. Pathol. 179 (2011) 2162–2168, https://doi.org/10.1016/j.ajpath.2011.07.010.
[37] X. Jin, Y. Sun, H. Yang, J. Li, S. Yu, X. Chang, Z. Lu, J. Chen, Deregulation of the MiR-193b-KRAS axis contributes to impaired cell growth in pancreatic cancer, PLoS One 10 (2015), https://doi.org/10.1371/journal.pone.0125515.
[38] H. Li, Y. Xu, W. Qiu, D. Zhao, Y. Zhang, Tissue miR-193b as a novel biomarker for patients with ovarian cancer, Med. Sci. Mon. Int. Med. J. Exp. Clin. Res. 21 (2015) 3929–3934, https://doi.org/10.12659/MSM.895407.
[39] H.E. Rauhala, S.E. Jalava, J. Isotalo, H. Bracken, S. Lehmusvaara, T.L.J. Tammela, H. Oja, T. Visakorpi, miR-193b is an epigenetically regulated putative tumor suppressor in prostate cancer, Int. J. Cancer 127 (2010) 1363–1372, https://doi.org/10.1002/ijc.25162.
[40] C. Xu, S. Liu, H. Fu, S. Li, Y. Tie, J. Zhu, R. Xing, Y. Jin, Z. Sun, X. Zheng, MicroRNA-193b regulates proliferation, migration and invasion in human hepatocellular carcinoma cells, Eur. J. Cancer 46 (2010) 2828–2836, https://doi.org/10.1016/j.ejca.2010.06.127.
[41] H. Jiménez-Wences, Di.N. Martínez-Carrillo, O. Peralta-Zaragoza, G.E. Campos-Viguri, D. Hernández-Sotelo, M.A. Jiménez-López, J.G. Muñoz-Camacho, V. H. Garzón-Barrientos, B. Illades-Aguiar, G. Fernández-Tilapa, Methylation and expression of miRNAs in precancerous lesions and cervical cancer with HPV16 infection, Oncol. Rep. 35 (2016) 2297–2305, https://doi.org/10.3892/or.2016.4583.
[42] M. Kara, O. Yumrutas, O. Ozcan, O.I. Celik, E. Bozgeyik, I. Bozgeyik, S. Tasdemir, Differential expressions of cancer-associated genes and their regulatory miRNAs in colorectal carcinoma, Gene 567 (2015) 81–86, https://doi.org/10.1016/j.gene.2015.04.065.
[43] K. Wu, Z. Zhao, J. Ma, J. Chen, J. Peng, S. Yang, Y. He, Deregulation of miR-193b affects the growth of colon cancer cells via transforming growth factor-β and regulation of the SMAD3 pathway, Oncol. Lett. 13 (2017) 2557–2562, https://doi.org/10.3892/ol.2017.5763.
[44] Q. Zhong, T. Wang, P. Lu, R. Zhang, J. Zou, S. Yuan, miR-193b promotes cell proliferation by targeting Smad3 in human glioma, J. Neurosci. Res. 92 (2014) 619–626, https://doi.org/10.1002/jnr.23339.
[45] S. Caramuta, S. Egyházi, M. Rodolfo, D. Witten, J. Hansson, C. Larsson, W.O. Lui, MicroRNA expression profiles associated with mutational status and survival in malignant melanoma, J. Invest. Dermatol. 130 (2010) 2062–2070, https://doi.org/10.1038/jid.2010.63.
[46] M. Lenarduzzi, A.B.Y. Hui, N.M. Alajez, W. Shi, J. Williams, S. Yue, B. O'Sullivan, F.F. Liu, MicroRNA-193b enhances tumor progression via down regulation of neurofibromin 1, PLoS One 8 (2013), https://doi.org/10.1371/journal.pone.0053765.
[47] M.L. Slattery, J.S. Herrick, L.E. Mullany, E. Wolff, M.D. Hoffman, D.F. Pellatt, J. R. Stevens, R.K. Wolff, Colorectal tumor molecular phenotype and miRNA: expression profiles and prognosis, Mod. Pathol. 29 (2016) 915–927, https://doi.org/10.1038/modpathol.2016.73.

[48] M.A. Blasco, Telomeres and human disease: ageing, cancer and beyond, Nat. Rev. Genet. 6 (2005) 611–622, https://doi.org/10.1038/nrg1656.
[49] M. García-Cao, R. O'Sullivan, A.H.F.M. Peters, T. Jenuwein, M.A. Blasco, Epigenetic regulation of telomere length in mammalian cells by the Suv39h1 and Suv39h2 histone methyltransferases, Nat. Genet. 36 (2004) 94–99, https://doi.org/10.1038/ng1278.
[50] R. Benetti, M. García-Cao, M.A. Blasco, Telomere length regulates the epigenetic status of mammalian telomeres and subtelomeres, Nat. Genet. 39 (2007) 243–250, https://doi.org/10.1038/ng1952.
[51] M.A. Blasco, The epigenetic regulation of mammalian telomeres, Nat. Rev. Genet. 8 (2007) 299–309, https://doi.org/10.1038/nrg2047.
[52] R. Firestein, X. Cui, P. Huie, M.L. Cleary, Set domain-dependent regulation of transcriptional silencing and growth control by SUV39H1, a mammalian ortholog of Drosophila su(var)3-9, Mol. Cell Biol. 20 (2000) 4900–4909, https://doi.org/10.1128/mcb.20.13.4900-4909.2000.
[53] A. Baniahmad, C. Steiner, A.C. Köhne, R. Renkawitz, Modular structure of a chicken lysozyme silencer: involvement of an unusual thyroid hormone receptor binding site, Cell 61 (1990) 505–514, https://doi.org/10.1016/0092-8674(90)90532-J.
[54] E.M. Klenova, R.H. Nicolas, H.F. Paterson, A.F. Carne, C.M. Heath, G.H. Goodwin, P.E. Neiman, V. v Lobanenkov, CTCF, a conserved nuclear factor required for optimal transcriptional activity of the chicken c-myc gene, is an 11-Zn-finger protein differentially expressed in multiple forms, Mol. Cell Biol. 13 (1993) 7612–7624, https://doi.org/10.1128/mcb.13.12.7612-7624.1993.
[55] A.A. Vostrov, M.J. Taheny, W.W. Quitschke, A region to the N-terminal side of the CTCF zinc finger domain is essential for activating transcription from the amyloid precursor protein promoter, J. Biol. Chem. 277 (2002) 1619–1627, https://doi.org/10.1074/jbc.M109748200.
[56] G.N. Filippova, C.P. Thienes, B.H. Penn, D.H. Cho, Y.J. Hu, J.M. Moore, T. R. Klesert, V.v. Lobanenkov, S.J. Tapscott, CTCF-binding sites flank CTG/CAG repeats and form a methylation-sensitive insulator at the DM1 locus, Nat. Genet. 28 (2001) 335–343, https://doi.org/10.1038/ng570.
[57] A.T. Hark, C.J. Schoenherr, D.J. Katz, R.S. Ingram, J.M. Levorse, S.M. Tilghman, CTCF mediates methylation-sensitive enhancer-blocking activity at the H19/Igf2 locus, Nature 405 (2000) 486–489, https://doi.org/10.1038/35013106.
[58] K. Tanimoto, A. Sugiura, A. Omori, G. Felsenfeld, J.D. Engel, A. Fukamizu, Human β-globin locus control region HS5Contains CTCF- and developmental stage-dependent enhancer-Blocking Activity in Erythroid Cells, Mol. Cell Biol. 23 (2003) 8946–8952, https://doi.org/10.1128/mcb.23.24.8946-8952.2003.
[59] J.E. Phillips, V.G. Corces, CTCF: master weaver of the genome, Cell 137 (2009) 1194–1211, https://doi.org/10.1016/j.cell.2009.06.001.
[60] N. Engel, J.L. Thorvaldsen, M.S. Bartolomei, CTCF binding sites promote transcription initiation and prevent DNA methylation on the maternal allele at the imprinted H19/Igf2 locus, Hum. Mol. Genet. 15 (2006) 2945–2954, https://doi.org/10.1093/hmg/ddl237.
[61] M.M. Franco, A.R. Prickett, R.J. Oakey, The Role of CCCTC-binding factor (CTCF) in genomic imprinting, development, and reproduction, Biol. Reprod. 91 (2014), https://doi.org/10.1095/biolreprod.114.122945.
[62] N.S.S. Naveh, D.F. Deegan, J. Huhn, E. Traxler, Y. Lan, R. Weksberg, A. Ganguly, N. Engel, J.M. Kalish, The role of CTCF in the organization of the centromeric 11p15 imprinted domain interactome, Nucleic Acids Res. 49 (2021) 6315–6330, https://doi.org/10.1093/nar/gkab475.
[63] M.E. Donohoe, L.F. Zhang, N. Xu, Y. Shi, J.T. Lee, Identification of a Ctcf Cofactor, Yy1, for the X chromosome binary switch, Mol. Cell 25 (2007) 43–56, https://doi.org/10.1016/j.molcel.2006.11.017.
[64] N. Xu, M.E. Donohoe, S.S. Silva, J.T. Lee, Evidence that homologous X-chromosome pairing requires transcription and Ctcf protein, Nat. Genet. 39 (2007) 1390–1396, https://doi.org/10.1038/ng.2007.5.
[65] C.L. Tsai, R.K. Rowntree, D.E. Cohen, J.T. Lee, Higher order chromatin structure at the X-inactivation center via looping DNA, Dev. Biol. 319 (2008) 416–425, https://doi.org/10.1016/j.ydbio.2008.04.010.
[66] O. Weth, R. Renkawitz, CTCF function is modulated by neighboring DNA binding factors, Biochem. Cell. Biol. 89 (2011) 459–468, https://doi.org/10.1139/o11-033.
[67] J. Zlatanova, P. Caiafa, CCCTC-binding factor: to loop or to bridge, Cell. Mol. Life Sci. 66 (2009) 1647–1660, https://doi.org/10.1007/s00018-009-8647-z.
[68] J. Ziatanova, P. Caiafa, CTCF and its protein partners: divide and rule? J. Cell Sci. 122 (2009) 1275–1284, https://doi.org/10.1242/jcs.039990.
[69] K. Kitamura, D. Shida, S. Sekine, Y. Ahiko, Y. Nakamura, K. Moritani, S. Tsukamoto, Y. Kanemitsu, Comparison of model fit and discriminatory ability of the 8th edition of the tumor-node-metastasis classification and the 9th edition of the Japanese classification to identify stage III colorectal cancer, Int. J. Clin. Oncol. 26 (2021) 1671–1678, https://doi.org/10.1007/s10147-021-01955-3.